

Clifford Assisted Optimal Pass Selection for Quantum Transpilation

Siddharth Dangwal¹, Gokul Subramanian Ravi¹, Lennart Maximilian Seifert¹, and Frederic T. Chong^{1,2}

¹University of Chicago

²Super.tech (a division of ColdQuanta)

Abstract

The fidelity of quantum programs in the NISQ era is limited by high levels of device noise. To increase the fidelity of quantum programs running on NISQ devices, a variety of optimizations have been proposed. These include mapping passes designed to minimize circuit depth and the number of CNOT operations, or to choose the most reliable links for performing CNOT gates in a device with variable error rates. A variety of routing passes have also been proposed aimed at minimizing the SWAP operation overhead. This is followed by scheduling methods that aim to minimize program execution time. On top of this, standalone optimizations have been proposed that avoid crosstalk, mitigate measurement errors or eliminate correlated errors. These optimizations are usually incorporated into a quantum transpiler as a set of passes. Popular quantum transpilers such as those proposed by IBM Qiskit, Google Cirq and Cambridge Quantum Computing make use of these extensively.

However, choosing the right set of transpiler passes and the right configuration for each pass is a challenging problem. Transpilers often make critical decisions using heuristics since the ideal choices are impossible to identify without knowing the target application outcome. Further, the transpiler also makes simplifying assumptions about device noise that often do not hold in the real world. As a result, we often see counter-intuitive effects where the fidelity of a target application decreases despite using state-of-the-art optimizations.

To overcome this challenge, we propose OPTRAN, a framework for Choosing an Optimal Pass Set for Quantum Transpilation. OPTRAN uses efficiently classically simulable quantum circuits composed entirely of Clifford gates, that resemble the target application, to estimate how different optimization passes interact with each other in the context of the target application. OPTRAN then uses this information to choose the optimal combination of passes that maximizes the target application's fidelity when run on the actual device. Our experiments on IBM machines show that OPTRAN improves fidelity by 87.66% of the maximum possible limit over the baseline used by IBM Qiskit. We also propose low-cost variants of OPTRAN, called OPTRAN-E-3 and OPTRAN-E-1 that improve fidelity by 78.33% and 76.66% of the maximum permissible limit over the baseline at a 58.33% and 69.44% reduction in cost compared to OPTRAN respectively.

1. Introduction

Quantum computers are capable of solving important problems like factorization [25], Hamiltonian simulation [14] or unordered search [12] much faster than classical computers that take impractically long times to solve these for large instances. Quantum computers make use of superposition, entanglement, and interference to achieve speed-ups over their classical counterpart. However, for most of these applications, we require fault-tolerant quantum computers where errors can be suppressed arbitrarily well using error correction codes [18]. These error correction codes require millions of qubits with substantially low physical error rates for any practically meaningful problem in the near future. In the meantime, we are looking for useful applications that can be run on current noisy quantum computers with roughly hundreds of qubits. These devices are said to operate in the Noisy Intermediate Scale Quantum (NISQ) [20] regime. Since these devices are resource-constrained, we suppress noise on these devices using error-mitigating optimization techniques aided by lightweight heuristics.

Many of these heuristics-based circuit optimizations like Noise Adaptive mapping [15], Sabre routing [13] or dynamical decoupling pulses [19] can be integrated into the transpilation pipeline as transpiler passes. A natural question that arises in such a setting is that of identifying the optimal set of optimization passes (and their specific configurations) that maximize the fidelity for an arbitrary quantum circuit on an arbitrary quantum device. Naively, these passes are often viewed as default utilities that improve the fidelity of almost every quantum circuit. However, there are many instances of practical/useful circuits for which these passes produce detrimental effects. These can vary widely according to the pass, the target circuit and the quantum device of choice. Further, the extent to which a transpiler pass improves fidelity is not well defined for any arbitrary circuit. Many passes that accomplish the same high-level task (for example mapping an application to a quantum device) may boost circuit fidelity by vastly varying magnitudes. The studies describing these passes are often highly empirical in nature and only evaluate improvements on a limited set of representative benchmarks. This makes choosing the best set of passes for an arbitrary quantum program a non-trivial task. This task gets further complicated when we consider the interaction between multiple passes in the transpilation pipeline. We observe from experiments that multiple passes used in conjunction produce effects that are vastly

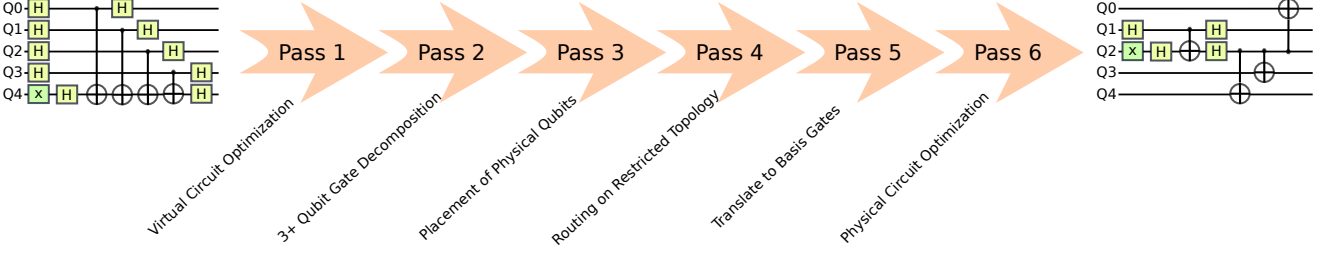


Figure 1: The IBM-Qiskit transpiler pipeline. The details of each of the passes have been mentioned in [Section 2.2](#). The transpiler takes an abstract quantum circuit as input and produces an optimized physical quantum circuit as an output.

different from their standalone effects. There may be cases where multiple passes that individually boost a circuit’s fidelity may hamper it when used together. This makes choosing the optimal set of transpiler optimization passes that maximize a target circuit’s fidelity a challenging task. Even for a given circuit, the optimal set of passes varies across quantum devices and over time. All these effects warrant the need to design a prediction framework to obtain a set of fairly optimal passes that transpiles an arbitrary circuit to maximize its fidelity on a particular device at some particular time.

We show that existing prediction tools like Estimated Success Probability (ESP) [27], or noisy simulators [4] are insufficient in this regard. These tools often use old characterization data to make predictions and/or do not model the noise in a quantum device accurately. As a result, the predicted fidelity is vastly different from the results we obtain when executing on a real quantum device.

To overcome this practical challenge, we propose OPTRAN, a framework to choose an optimal set of passes from multiple possible candidates to maximize circuit fidelity. OPTRAN takes the set of input standalone passes and generates all feasible pass combinations (though this number can be limited through partial heuristics), followed by transpiling the target application circuit using each of these combinations. It then creates Clifford Dummy circuits for each of these post-transpilation application circuits, which are composed entirely of Clifford gates with structures similar to the original post-transpilation circuits. This makes the Clifford Dummy circuits efficiently classically simulable [11]. Because of the high structural similarity, the Clifford Dummy circuits suffer from similar noise effects as the original circuit, which we show empirical evidence for. OPTRAN then determines the pass combination that maximizes the fidelity of the Clifford Dummy circuits by executing them on a real device as well as a noiseless simulator. This is only for the Dummy circuits but not for the original application since it does not consist of only Clifford gates. Since the dummy circuits and original circuits are similar in structure and suffer from similar noise, the OPTRAN hypothesis is that the optimal pass set for the Clifford dummy circuit is effective for the original application circuit as well. We provide a variety of benchmark results that confirm this hypothesis.

OPTRAN key contributions, insights and results:

1. We show that the fidelity of an arbitrary quantum circuit varies substantially when transpiled using different optimization pass combinations. Further, the optimal pass combination is difficult to determine using a characterization-based approach since it varies by input circuit, time and execution device.
2. We observe that existing prediction mechanisms like ESP and Noisy simulations are insufficient for the task described above.
3. OPTRAN uses appropriate Clifford Dummy circuits to choose the best pass combination for any arbitrary circuit.
4. The average fidelity increase by OPTRAN over the baseline is equal to 87.66% of the maximum permissible value. The default compilation mechanism used by Qiskit recovers only 55% of the maximum achievable fidelity.
5. Further, we propose low-cost variants of OPTRAN called OPTRAN-E-3 and OPTRAN-E-1, that increase fidelity by 78.33% and 76.66% of the maximum permissible limit at 58.33% and 69.44% cost reduction compared to OPTRAN respectively. As opposed to OPTRAN, that scales exponentially in the number of compiler stages, OPTRAN-E-1 and OPTRAN-E-3 show a linear scaling.

2. Background

2.1. Qubits and Quantum Gates

The smallest unit of computation in a quantum program is [n](#) the quantum bit, or qubit. Unlike a classical bit that is either 0 or 1 at any particular point in the computation, a qubit can exist as a superposition of these states. The most general state of a qubit is given as $|\psi\rangle = \alpha|0\rangle + \beta|1\rangle$, where α and β are complex numbers, such that $|\alpha|^2 + |\beta|^2 = 1$.

Qubits are acted upon by quantum gates to accomplish quantum computation. This is followed by measurement, that collapses a qubit in superposition to either 0 or 1. On current NISQ-era machines, these gates and measurement operations are noisy, with two-qubit operations being much more noisy than single-qubit operations. For example, on the five-qubit IBMQ-Lima quantum computer, the average CNOT error rate is around 1.2% and the average measurement error rate is around 2.6% [1]. Further, these error rates are highly spatially variable and vary drastically according to the coupler and the qubit that is chosen. Temporal variations are also observed in

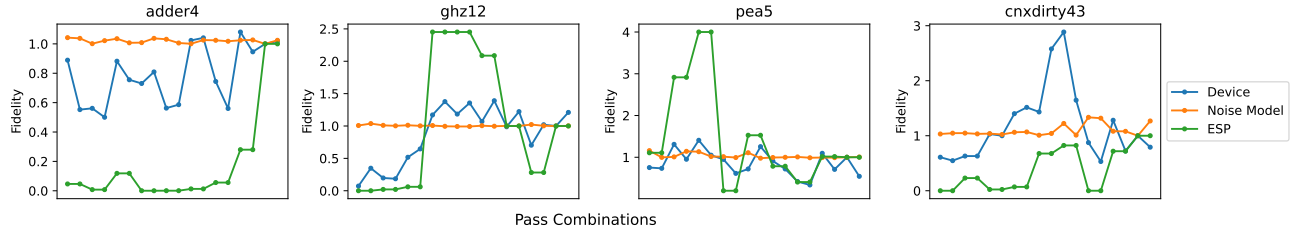


Figure 2: Fidelity trends for device execution, noise model and ESP for four workloads - adder4, ghz12, pea5 and cnxdirty43

these error rates.

2.2. Quantum transpilation

The way a quantum program is compiled is very similar to a classical program. The transpiler takes a quantum circuit as input and applies a set of transformations (called transpiler passes) to produce an executable that respects the constraints of a specific device (for instance qubit connectivity and native gate set) and ideally minimizes the expected error. One can also include certain optional passes that purely aim to improve circuit fidelity. One of the most popular quantum transpilers, the IBM Qiskit transpiler accomplishes this in six broad steps [4], which are shown in Figure 1 and explained in the following:

- **Virtual Circuit Optimization:** Often, basic linear algebra identities can be used to convert multiple single qubit gates into one gate. For example, a sequence of Hadamard (H), followed by Pauli-Z (Z), followed by Hadamard (H), can be replaced by a single X gate ($HZH = X$). Many other similar identities exist that can be used to reduce the gate count in a circuit. Since every gate potentially introduces noise into the system, reducing the total gate count by applying these transformations is desirable.
- **3+ Qubit Gate Decomposition:** Typically superconducting quantum hardware can support only single- and two-qubit gates on qubits. Thus, gates that act on more than two qubits need to be decomposed as a combination of single- and two-qubit gates. Such decompositions are guaranteed to exist according to the Solovay-Kitaev theorem [7].
- **Placement on Physical Qubits:** The virtual (logical) qubits in an abstract quantum circuit need to be mapped to the physical qubits (hardware implementations) on an actual quantum device. Depending on the qubits chosen and the order they are used in, the fidelity of the circuit execution changes as different qubits have different lifetimes and experience different gate errors. Appropriate mapping can help minimize the use of highly error-prone qubits and inter-qubit links.
- **Routing on Restricted Topology:** An actual quantum device often does not have all-to-all device connectivity. Thus, two qubits that have a gate between them in the abstract circuit and are not mapped adjacent to each other on the actual device need to be routed adjacent to each other. This is accomplished using SWAP gates. Because two-qubit gates

are typically the dominating source of error in quantum hardware, a SWAP operation (equivalent to three CNOTs) is very expensive. A good routing pass tries to minimize the number of necessary SWAP gates and chooses swap paths with minimal two-qubit gate error.

- **Translate to Basis Gates:** Any quantum device has a set of basis gates that can be executed on it. This basis set is chosen such that any arbitrary quantum gate can be expressed as a combination of its constituent elements. Thus, this step involves taking all quantum gates in the hardware-mapped quantum circuit and decomposing them into elements of the basis gate set.
- **Physical Circuit Optimization:** Oftentimes, one can apply certain optimizations to the hardware-mapped quantum circuit so as to increase the chances of correct execution. Examples include padding the idle spaces in a quantum circuit with dynamical decoupling pulses [19] and serializing CNOTs with high crosstalk between them [16]. Crosstalk is a type of noise that appears when two-qubit gates are executed close to each other in parallel. Post this final step, the circuit is ready to be executed on a device.

2.3. Transpiler Passes for Fidelity Improvement

In the past, numerous transpiler passes have been proposed to combat a variety of errors. The first strategy to improve circuit fidelity is to map qubits close to each other to reduce routing overhead. Routing requires SWAP gates, each of which is composed of three CNOT gates. This makes them extremely error-prone. For example, in IBMQ-Lima, the error rate of a SWAP gate is around 3.5%. Dense mapping, used by the IBM-Qiskit transpiler, chooses the most densely connected subgraph with the same number of qubits as the quantum program and maps the program to this subgraph. An alternate strategy called Noise-Adaptive mapping takes into account the variable error rates of CNOT links and measurements and chooses the mapping that uses CNOTs and measurements with the highest fidelities [15,27] in a greedy fashion. Another strategy called SABRE starts with random mapping. It iteratively computes the expected SWAP routing cost for the current mapping and updates it to reduce this cost [13]. In cases where all CNOT links in the device have similar error rates, dense mapping tends to be the best strategy since it minimizes the number of SWAPs. In cases where certain CNOTs are substantially worse than others, Noise-Aware mapping tends to be a

good choice since it actively avoids error-prone CNOTs often at the cost of increased SWAP count. SABRE makes use of a user-defined heuristic cost function to determine the cheapest SWAPs needed for a particular initial mapping. Starting with a random mapping, it is iteratively refined to arrive at a good initial mapping that also has an inexpensive routing cost. None of the two cost functions that SABRE proposes [13] take the variability in CNOT error rates into account. However, it is quite fast and searches the space of possible routing strategies effectively. Thus, in cases where there is not much variability in CNOT error rates and where the problem size is large, SABRE tends to do well.

Several routing policies have also been proposed that specifically aim to minimize the number of swap gates in a circuit. These include stochastic routing, basic routing, and SABRE routing. Stochastic routing is a brute force hit-or-miss strategy where the router inserts random swaps between qubits not connected to each other. The pass terminates when it finds a configuration that places all logically interacting qubits next to each other at the right time instances. Since this search does not have a guiding principle, the results can vary substantially across runs. However, by keeping the seed constant during this stochastic process, we can guarantee the reproducibility of results. Basic routing finds the shortest route between two non-interacting qubits, routes them along that path, and takes them back to their initial positions.

There also exist policies that break the transpilation flow abstraction to achieve a reduction in gate count. Trios [8] does not decompose three-qubit Toffoli gates into single- and two-qubit gates in step 2 of the transpilation flow described in Section 2.2. Instead, it maps and routes a Toffoli gate like any other gate and finally decomposes it into basis gates in step 5. This leads to a reduction in gate count and circuit depth, and consequently an improvement in circuit fidelity.

Several optimization passes have also been proposed that can easily be incorporated as part of the transpilation pipeline. This includes software strategies to mitigate crosstalk [16] and padding the circuit with dynamical decoupling pulses [5, 21].

3. Motivation

If we get rid of all physical and logical circuit optimizations and assume that the transpiler uses the most optimal basis gate decomposition, one can choose from a variety of mapping, routing, and scheduling passes to transpile the circuit. We study the variation of the “best” mapping-routing-scheduling (M-R-S) combination over time across different circuits and machines.

3.1. Variation of Optimal Pass Combination for Transpilation

The IBM-Qiskit transpiler has four inbuilt mapping options: trivial, dense, noise-adaptive and sabre. The trivial mapping option simply maps virtual qubit i in the circuit to physical qubit i in the device. The dense mapping pass aims to mini-

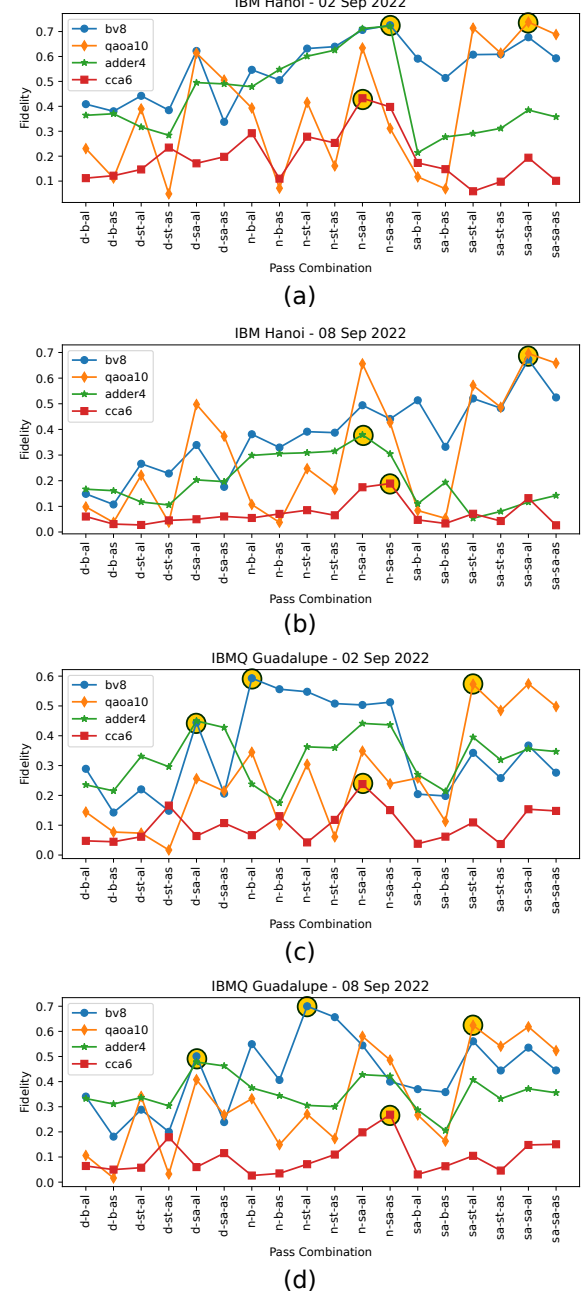


Figure 3: Variation of optimal mapping-routing-scheduling pass set for four circuits on IBM Hanoi and IBMQ Guadalupe on 2 Sep 2022 and 8 Sep 2022. The best pass combination in each subplot is highlighted with a yellow circle.

imize the number of SWAP operations by mapping the circuit to the most densely connected subgraph of the machine. The noise-adaptive pass uses the device characterization data to map qubits such that the circuit uses the most reliable links to execute CNOT gates. Sabre also proposes a novel scheme that aims to minimize the number of CNOT gates and reduce circuit infidelity. The transpiler also offers four routing options, i.e. basic swap, stochastic swap, look-ahead swap and

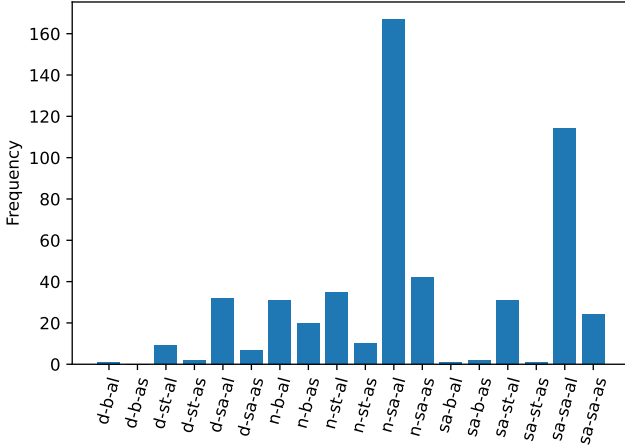


Figure 4: Frequency of different optimal M-R-S combinations, when computed over 4 device backends, 13 days and 13 circuits.

sabre swap, and two scheduling options - As Late As Possible (ALAP) and As Soon As Possible (ASAP). Readers can refer to [2] for details about these passes. Although Qiskit uses Sabre mapping, Sabre routing and ALAP scheduling for its highest optimization level (optimization_level = 3), this often is not the best policy.

To understand the variation of the best M-R-S combination, we take four circuits, compile each one using different M-R-S combinations and run them on multiple IBM machines. For this study, we do not use trivial mapping and look-ahead swap. Trivial mapping, as the name suggests is a very naive strategy and is subsumed by other strategies for any proxy metric for fidelity (like minimizing CNOTs or choosing the most error-resilient CNOTs). Lookahead swap although useful fails to produce an output for many of our benchmarking circuits. Thus, we get a total of 18 different M-R-S combinations (3 mappers, 3 routers, and 2 schedulers).

Figure 3 shows how the optimal transpiler pass set varies for different circuits. There is substantial variation in the optimal transpiler pass set across different circuits and devices on a given date. We also observe that the optimal pass set varies for the same circuit and device depending on the date of execution. This is expected since each device has different noise characteristics that also drift with time.

We also observe that there is a substantial spread in the optimal M-R-S combination. Figure 4 shows the variation of optimal M-R-S combination for a set of thirteen circuits, executed on four machines across thirteen days. While noise-adaptive-sabre-alap and sabre-sabre-alap (used in Qiskit optimization_level_3) are the two most frequent sets, we see a non-zero probability of occurrence for a variety of other pass sets too.

3.2. Pass Interactions

The problem of choosing the optimal pass set for transpiling an arbitrary quantum circuit is made further complicated by

the way these passes interact with each other. If we go by pure intuition, we would expect that two passes that improve fidelity over the baseline would work in synergy to boost it further. Similarly passes that are detrimental and perform worse than the baseline would also combine to produce a result that is worse compared to the baseline. A combination of a “good” and a “bad” pass might or might not improve fidelity depending on which pass dominates. However, that is often not the case.

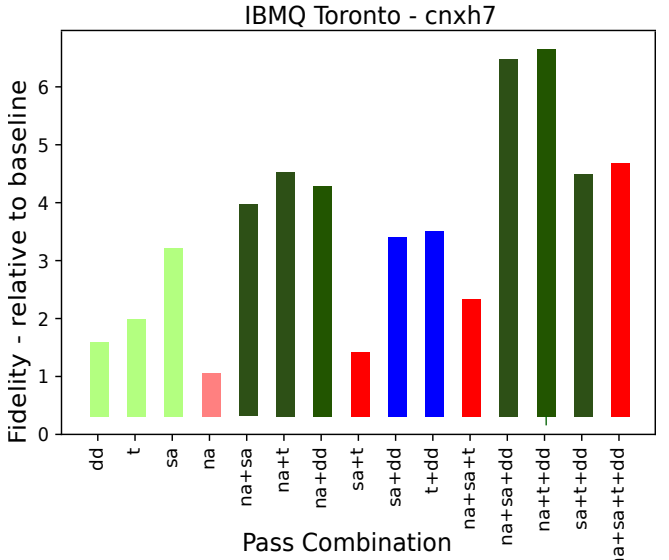


Figure 5: Pass Interactions for 7 qubit Halfdirty Multicontrol (cnxh7) CNOT on IBMQ-Toronto

Figure 5 gives an example of how passes interact in the case of the circuit cnxh7 on IBMQ-Toronto. It is a multi-control CNOT circuit, the details of which can be found in Table 3. We choose a baseline where we transpile the circuit using dense mapping, stochastic routing and alap scheduling. We then test four passes - Noise-Adaptive mapping, Sabre routing, Trios and Dynamical Decoupling compared to this baseline. We see that Noise Adaptive Mapping (na) standalone degrades circuit fidelity. The fidelity it produces relative to baseline is less than 1, signaling a downgrade. However, when combined with Dynamical Decoupling (dd) and Trios (t), it produces the highest fidelity across all pass combinations. Compare this with Sabre, which standalone gives a 3x improvement over the baseline, and Trios which alone gives a 2x improvement over the baseline, but together they give no fidelity improvement over the baseline (sa+t ~ 1x). Similarly, sabre when combined with na+t+dd reduces the fidelity despite improving it standalone. In Figure 5, the dark-red bars show “destructive interference”, where the net result of the combination potentially improves when we take away one of the constituent passes of the combination. The dark-green bars show all cases of “constructive interference”. This refers to all cases where the combined effect of a set of passes is greater than the sum

of the improvements caused by the constituents. The blue bars represent cases, where the net effect is broadly the same as that of one of its constituents.

3.3. Existing Prediction Tools

There are a variety of metrics and tools to estimate the fidelity of a circuit before executing it on a device. The most elementary one is Estimated Success Probability (ESP). ESP multiplies gate reliabilities ($r_i = 1 - \text{gate error rate}_i$), qubit measurement reliabilities ($m_i = 1 - \text{measurement error rates}_i$) and decoherence reliability ($r_t = \exp(-\frac{t}{T_1} - \frac{t}{T_2})$) to get an estimate of the success of program execution. $ESP = \prod_i (r_{xi}) \prod_j (r_{mj}) r_T$. The error rates are obtained from device calibration data. This metric, although extremely fast to compute, ignores phenomena like crosstalk and drift. The error rates from the calibration cycle get outdated very quickly due to high drift in these devices and give inaccurate probability estimates.

We could also run a noisy simulation of the circuit on a classical computer to estimate the fidelity. This is the most advanced prediction tool available to us. However, even a full noisy circuit simulation gives extremely poor predictions of the best M-R-S combination. This is primarily because the simulator uses outdated calibration data and does not model complex noises in the device. Further, the noisy simulator is non-scalable, which makes it a non-feasible solution as circuit sizes grow.

Figure 2 shows how the fidelity of four workloads varies with different M-R-S combinations when run on an actual quantum device, noise model or computed using ESP. We perform the device experiments on IBMQ Guadalupe. ESP and Noise Model trends have a poor correlation with actual device trends and are not good predictors.

4. OPTRAN: Design

To identify the transpiler pass combination that maximizes program fidelity, we propose OPTRAN. OPTRAN can be implemented as a transpiler pass and be readily integrated with the existing passes in popular quantum transpilers like IBM-Qiskit, Google Cirq and tket. Other than mapping, routing and scheduling passes, OPTRAN can also be used to decide whether to apply a heuristic-based optional optimization pass on a circuit or not in order to maximize fidelity.

4.1. OPTRAN: Overview

As part of OPTRAN, we perform the following steps to determine the best transpiler pass combination for an arbitrary input circuit:

1. Transpile the circuit for all possible pass combinations and store all the post-transpilation circuits. If there are n steps in the transpiler and step i has a_i choices, then the total number of circuits would be $\prod_{i=1}^n a_i$. For example, if step i is the mapping pass then the possible options are ‘dense’, ‘noise adaptive’ or ‘sabre’ that gives us a value $a_i = 3$. If step i is a binary optimization pass - for example,

application of DD, then the two options are the application of DD or non-application of DD that gives us a value $a_i = 2$.

2. Create a Clifford Dummy circuit for each of these $\prod_{i=1}^n a_i$ circuits. These circuits are made entirely out of Clifford gates. As a result, they can be simulated on a classical computer in polynomial time [3]. For each non-Clifford gate in any of the post-compilation circuits, we replace it with the “closest” Clifford gate. We leave the Clifford gates in the original circuit unchanged.
3. We simulate these $\prod_{i=1}^n a_i$ Clifford Dummy circuits on a classical computer, that gives us the noiseless distribution for each of them. We also run these on a NISQ device to obtain a noisy distribution. Using the noiseless distributions, we determine the transpiler pass combination that gives us the highest fidelity on the NISQ device. Let us call this pass combination P^* .
4. From the set of original post-transpilation circuits, we choose the circuit that had been transpiled using P^* and run it on the NISQ device to maximize the fidelity of circuit execution.

Figure 6 shows an overview of the entire scheme.

4.2. Creation of Clifford Dummy Circuits

In the IBM-Qiskit transpiler, a circuit is expressed as a combination of the basis gates post transpilation Id, X, SX, RZ, CNOT. All these gates are Clifford gates except the RZ gate. This is a parameterized gate that rotates a qubit around the Z-axis by the input parameter (θ). If this parameter is in $\{\frac{\pi}{2}, \pi, \frac{3\pi}{2}, 2\pi\}$, the resulting gate is Clifford. For all values in between, we round it to the nearest multiple of $\frac{\pi}{2}$. For parameter values that are close to multiples of $\frac{\pi}{4}$ ($|\theta - \frac{n\pi}{4}| < \delta$), where δ is a design parameter that we have chosen to be $\frac{\pi}{100}$ and $n \in \{1, 3, 5, 7\}$, we round the parameter to $\frac{(n+1)\pi}{4}$ or $\frac{(n-1)\pi}{4}$ randomly. This process is repeated multiple times with the objective of creating a Clifford circuit with as many peaks in the output distribution as there are in the original circuit. If we fail to get such a circuit, we choose one where the number of peaks is closest to that in the original. Although this method is applicable exclusively to the IBM-Qiskit transpiler, we can design similar strategies for other output basis sets.

4.3. Why do Clifford Dummy Circuits Work?

Structurally, Clifford Dummy Circuits are similar to the original circuit. The major source of error in a circuit is CNOT gates. CNOT gate errors and crosstalk are significantly higher than that due to their single-qubit counterparts [22]. Since CNOT is a Clifford gate, the number and position of CNOTs are the same in the original and Clifford Dummy Circuit. Some Passes that we consider have qubit-state-dependent effects. For example, the effect of Dynamical Decoupling on a qubit depends on the state it is in. Thus, we change the parameter of the RZ gate by the smallest amount possible so that the similarity of the qubit state at intermediate positions in the circuit is maximized. We quantify this by checking the cor-

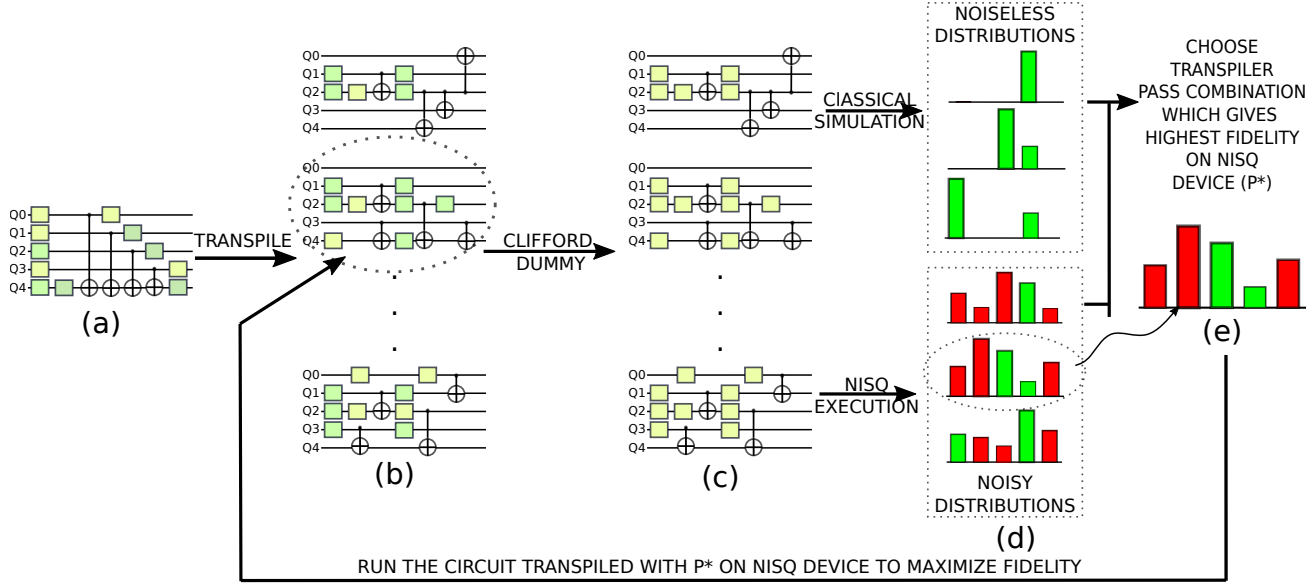
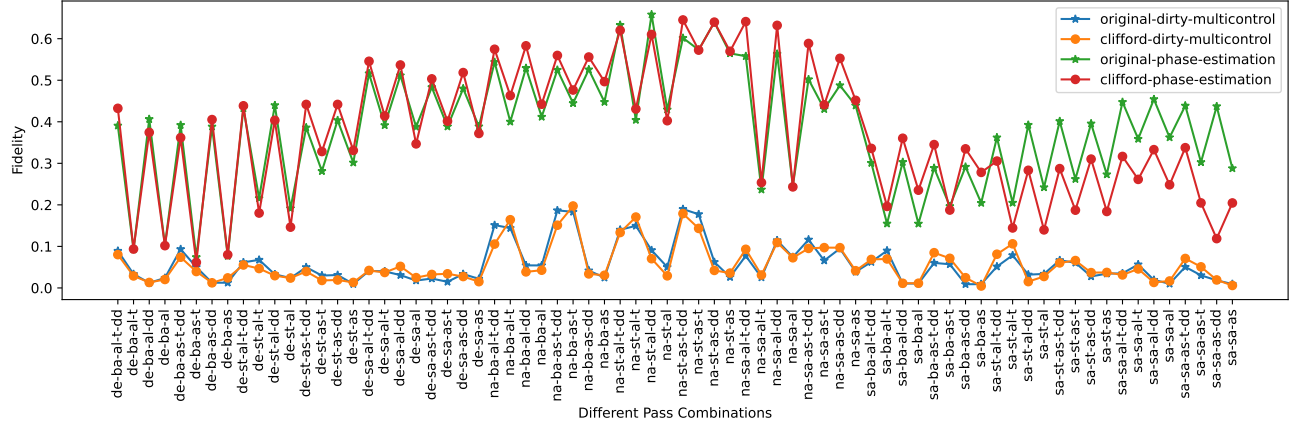


Figure 6: OPTRAN Overview: (a) Input Circuit (b) Post-Transpilation Circuits. Each circuit has been transpiled using one element of the set of all possible transpiler pass combinations. (c) Clifford Dummy Circuits. For each of the post-transpilation circuits in step (b), we create a Clifford dummy circuit that is classically simulable. (d) We run each Clifford Dummy Circuit on a noiseless classical simulator and also on a NISQ machine. Using the noiseless distributions, we estimate which transpiler pass combination gives the highest fidelity on a NISQ machine. Let this pass combination with P^* . Out of all the circuits in step (b), we choose the one transpiled using P^* to maximize fidelity.



relation between the variation of fidelity with transpiler pass combination in the original and dummy circuits. In most cases, the correlation is extremely strong. Even in cases where it is weak due to a few spurious points, the fidelity of the original and dummy circuit is maximized for the same transpiler pass combination. Figure 7 shows the fidelity trend for the Original circuits and Clifford Dummy circuits for two benchmarks: phase estimation and dirty-multicontrol on IBMQ Toronto. Table 1 lists the correlation values between the original circuit and Clifford Dummy circuit for IBMQ Auckland.

4.4. Reduction in Cost

4.4.1. OPTRAN-E

The cost of OPTRAN scales exponentially in the number of passes available at each step. If there are p steps in the transpilation pipeline and n_i options at step i , then the number of Clifford Dummy circuits we will have to create is $\prod_{i=1}^p n_i$. We have also seen how we cannot evaluate a pass in a standalone fashion since these passes often interact with other passes in counterintuitive ways. This warrants an exhaustive search across an exponential number of pass combinations to obtain the best pass combination. A drastically different strategy would be to choose passes in a greedy fashion. We choose the

Circuit	Correlation (%)
bv10	99.27
qaoa11	76.76
adder4	62.89
ghz12	99.70
cnx55	86.05
adder2	60.2
pea5	97.28
cnxdirty43	70.07
hs6	73.62
vqe10	71.74
pc5	89.85

Table 1: Correlation data for IBM Auckland

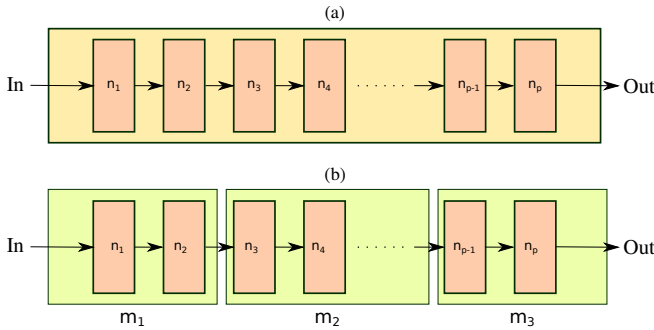


Figure 8: (a) Transpiler pipeline for OPTRAN. We optimize over all transpiler stages together. (b) Transpiler pipeline for OPTRAN-E. We break the pipeline into chunks (m_1, m_2, m_3) and choose the top-k options combinations from each stage to search for the optimal pass combinations.

“best pass” at each stage, fix it and then progress to choosing “best pass” at the next stage. This strategy would scale as $\sum_{i=1}^p n_i$, however it would give quite poor results because of the effect of pass interactions. We can, however, follow an intermediate strategy, where we split the transpilation pipeline into chunks comprising a few steps each. For each chunk, we obtain the top-k best combinations and use only these to evaluate the top-k pass combinations at the end of the next chunk. We do this until we reach the final chunk, where we choose just the top-1 (or best) pass combination. We call this strategy OPTRAN-E. If we break the pipeline into t chunks and each chunk consists of m_j steps where the number of possible pass options available at each step is n_i , then we the number of circuits we need are $\prod_{i=1}^{m_1} n_i + k \cdot \prod_{i=m_1}^{m_1+m_2} n_i + \dots + k \cdot \prod_{i=\sum_{j=1}^{t-1} m_j}^{\sum_{j=1}^t m_j} n_i$.

If we assume $n_i = n \forall i$, then the cost reduces to $\mathcal{O}(\frac{p \times n^t \times k}{t})$, which scales linearly in the number of pipeline stages, p . For our experiments, we will split the pipeline only into two steps. We choose the value of m_1 as 3 and m_2 as 2. The n_i values are - $n_1 = 3, n_2 = 3, n_3 = 2, n_4 = 2, n_5 = 2$, which reduces our expression of total circuits to $18 + 4k$.

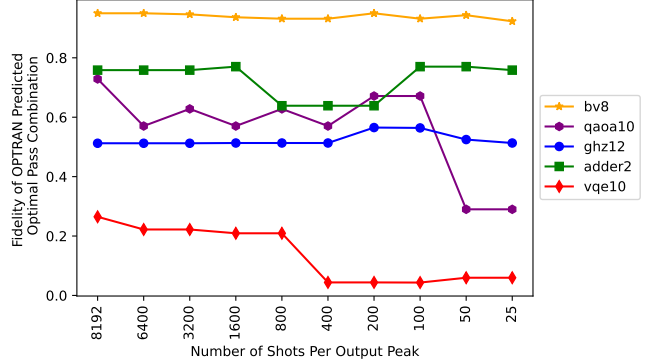


Figure 9: Variation of OPTRAN Predicted Optimal Pass Combination Fidelity with “Shots per Peak” on IBMQ Toronto.

4.4.2. Shot Reduction (SR)

While executing a circuit on a NISQ machine, we run it for multiple shots to infer the output correctly in the presence of errors. In IBM machines, the maximum allowable shots for a circuit is 8192. For multi-modal circuits, an increased number of shots is important to reduce statistical errors in order to get an output distribution which accurately represents the amplitudes in the final state of the quantum register, right before measurement. However, for the purpose of relative fidelity comparison, we do not need a very high number of shots. We can tolerate some error since we are not interested in the absolute fidelity numbers, but their relative order. Using this insight, we propose executing the Clifford Dummy circuits on the device for a reduced number of shots. We allocate a shot budget of 200 shots for every “peak” in the noise free ideal output distribution of a Clifford Dummy circuit. We have access to this noise free distribution since we can simulate Clifford Dummy circuits efficiently on a classical computer. This strategy of increasing the number of shots with the number of output peaks minimizes statistical errors in multi-modal distributions. We observe that this strategy leads to results at par with the baseline (where we use 8192 shots for every Clifford Dummy circuit), for drastically reduced overhead.

Figure 9 shows how the fidelity corresponding to the optimal pass combination as predicted by OPTRAN varies with the number of shots per peak for five workloads on IBMQ Montreal. Trends for OPTRAN-E-3, and OPTRAN-E-1 are similar. We can see that the trend is fairly stable up to 200 shots and starts wiggling a bit after that, even increasing in some cases. However, we take a conservative estimate and stick to 200 shots per-peak since it seems to generalize well.

4.5. Overhead

Currently OPTRAN requires the user to (a) compile a circuit for all possible pass combinations (Compilation Overhead), (b) create Clifford dummy circuits for every compiled circuit (Clifford Generation Overhead), (c) execute these circuits on a simulator (Simulation Overhead), and (d) execute the

Circuit	OPTRAN with SR	OPTRAN-E-1 with SR
bv8	1.75x	0.53x
qaoa10	1.75x	0.53x
ghz12	3.51x	1.06x
vqe10	3.51x	1.06x
hs6	2.39x	0.73x
qaoafm6	67.08x	20.49x

Table 2: Quantum Execution Overhead for OPTRAN-E, and OPTRAN-E-1 with Shot Reduction (SR). The overheads are reported as multiples of the baseline number of shots used to run a circuit (8192). Without Shot Reduction, the overheads for OPTRAN, and OPTRAN-E-1 are 72x, and 22x respectively.

same Clifford dummy circuits on actual hardware (Quantum Execution Overhead). The net overhead for all these steps is documented below. For steps (a)-(c), we provide the wall clock time since these steps are executed on a Classical computer. For (d), we provide the total number of shots needed to execute all Clifford Dummy circuits, and compare it with the number of shots used while executing the baseline (8192). The data is available in Table 3.

We can see that the overheads are fairly nominal compared to the potential fidelity improvement from OPTRAN. In all cases, the total classical overhead does not exceed one minute. In most cases, the quantum execution overhead for OPTRAN, and OPTRAN-E-1 is around 1.75x, and 0.53x respectively of the baseline cost (refer to Table 2). This is a substantial reduction from the 72x and 22x overhead that OPTRAN and OPTRAN-E-1 introduce respectively without shot reduction. The Clifford dummy simulation time is especially small, which is expected behavior.

5. Methodology

5.1. Benchmarks

We conduct our evaluations on a total of 19 circuits. These are given in Table 3. The circuit depths and number of qubits are chosen such that each benchmark has a baseline (qiskit - optimization_level_3) fidelity that is between 2% and 90%. We do that to ensure the applicability of OPTRAN for a wide variety of benchmarks, and not present fidelity gain only when baseline is negligibly low. The gate depth and size vary depending on the transpiler pass combination chosen and are presented in 3. The final evaluations are conducted on three IBM devices - IBMQ Toronto (27 Qubits), IBM Auckland (27 Qubits), and IBM Hanoi (27 Qubits).

5.2. Passes

For the purpose of this paper, we consider ten passes at different steps of the transpilation pipeline to get a total of 72 pass combinations. The passes are:

1. Mapping - Dense, Noise Adaptive, Sabre
2. Routing - Basic, Stochastic, Sabre

3. Scheduling - As Soon As Possible (ASAP), As Late As Possible (ALAP)
4. Optimization 1 - Trios
5. Optimization 2 - Dynamical Decoupling

Since mapping, routing, and scheduling are compulsory steps we choose one pass for each step, giving us 3, 3, and 2 choices at each step respectively. As the optimization passes are optional, we have two options for each pass: either apply the optimization or not. With two optimization passes, we get a total of four options. Thus, we have a total of $3 \times 3 \times 2 \times 2 \times 2 = 72$ possible combinations.

For OPTRAN, we search over all these 72 possible combinations. For OPTRAN-E, we split the pipeline into two chunks

1. Mapping + Routing + Scheduling (M-R-S)
2. Optimization 1 + Optimization 2 (O1-O2)

For step 2, we consider only the top-k pass combinations that we obtain from step 1. For our evaluations, we consider two values of the parameter ‘k’ - 1 and 3. Thus, we first select the top-1 (best)/top-3 best M-R-S pass combinations, before selecting the best M-R-S-O1-O2 combination from amongst these M-R-S combinations. We label these cases as ‘OPTRAN-E-1’ and ‘OPTRAN-E-3’ in our evaluations.

5.3. Infrastructure

We integrate OPTRAN as part of the Qiskit framework, right before the transpilation step. The Clifford dummy circuits help us choose the best pass combination that we use to transpile the original circuit and then execute on hardware.

5.4. Evaluation Comparisons

1. Opt3: The optimization_level_3 flag in the qiskit transpiler.
2. Opt3+DD+Trios: Transpilation with optimization_level_3 flag along with binary optimizations Trios and DD included.
3. ESP: Best fidelity predicted by ESP.
4. Noise Model: Best fidelity predicted by the Noise Model.
5. OPTRAN: Best fidelity predicted by our proposed method where we do an exhaustive search over all 72 combinations.
6. OPTRAN-E-1: Best fidelity predicted by our proposed method, where we first choose the top 1 (best) M-R-S combination without any binary optimizations. We fix this M-R-S combination when searching for the best pass combination.
7. OPTRAN-E-3: Best fidelity predicted by our proposed method, where we first choose the top 3 (best) M-R-S combinations without any binary optimizations. We fix the M-R-S combination from one among these when searching for the best pass combination.
8. Oracle: Highest possible fidelity for the circuit across all pass combinations. All fidelity numbers are reported as fraction of the oracle fidelities.

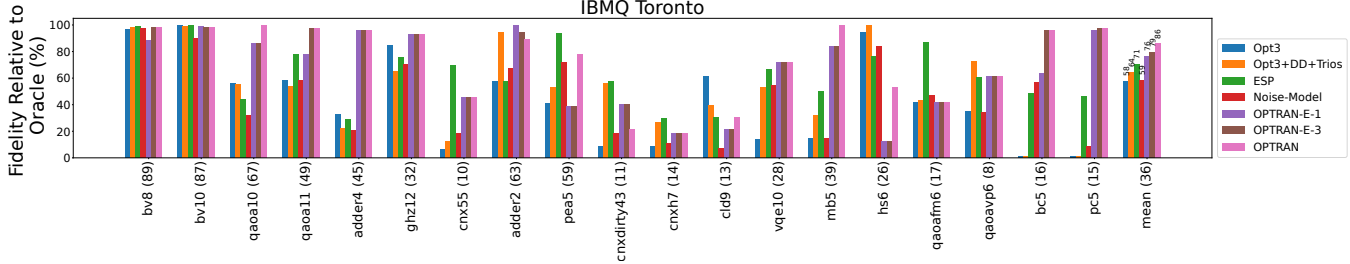


Figure 10: Fidelity Relative to Oracle evaluated on IBMQ Toronto

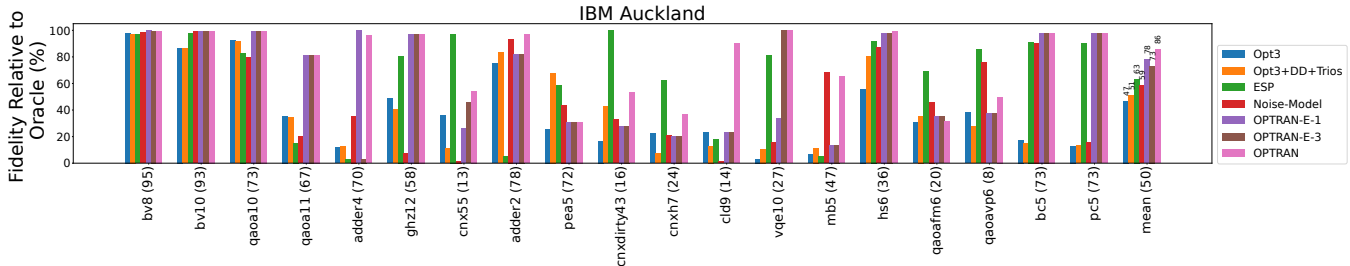


Figure 11: Fidelity relative to Oracle evaluated on IBM Auckland.

5.5. Evaluation Metrics

Fidelity relative to Oracle: We compute all fidelities using PST (Probability of Successful Trial). This metric has been used extensively in the past [26]. We define PST as the probability of obtaining any one of the bitstrings also present in the ideal distribution. $PST = \sum_{i \in S} p_i$ where S represents the keys in the ideal, noiseless distribution. Fidelity relative to oracle is defined as $fidelity_relative_to_oracle(M) = \frac{fidelity(M)}{fidelity(Oracle)}$, where M is the protocol we are testing. Since $fidelity(Oracle)$ is the best possible fidelity, the resulting number is bounded by 1 (or 100%).

6. Evaluation

Figures 10, 11 12, show the fidelities of the benchmark circuits for various evaluation modes on IBMQ Toronto, IBM Auckland, and IBM Hanoi respectively. The Oracle fidelities of all circuits (corresponding to the 100% mark in the figures) are reported along with the circuit name in the x-axis label. On all three devices, on average, OPTRAN, and OPTRAN-E outperform all other evaluation modes. There are cases where OPTRAN performs slightly poorly w.r.t. other evaluations, however this is mostly true for circuits with low oracle fidelities which results in the the absolute value of fluctuations being quite negligible. We could attribute most of these small fluctuations to statistical errors. Few other cases where OPTRAN is outperformed by other execution modes (For example qaoafm6 on IBMQ Toronto, and IBM Auckland) correspond to circuits with high variance distributions. High variance in circuit distributions makes it hard to get good correlations between the original circuit and its corresponding Clifford Dummy. Ref. [5] also points out similar effects. Another reason

On average, OPTRAN achieves 86% of the maximum achievable fidelity on IBMQ Toronto, going all the way upto 100% for many benchmarks. OPTRAN-E-3 and OPTRAN-E-1 recover on average 79% and 76% of the maximum achievable fidelity for a 58.33% and 69.44% reduction in cost, respectively.

On IBM Auckland, OPTRAN, OPTRAN-E-3, and OPTRAN-E-1 recover on average 86%, 73%, and 78% of the maximum achievable fidelity. On IBM Hanoi, these numbers are 91%, 83%, and 76% of the Oracle fidelity respectively. On these two devices too, the reduction in cost by OPTRAN-E-3, and OPTRAN-E-1 is 58.33% and 69.44% respectively.

7. Discussion

OPTRAN can be used with any heuristic that can be incorporated as a pass in the transpiler. Further, it can be used orthogonally to non-transpiler heuristics [6, 10, 26].

Past work has looked at solving the problem of choosing the optimal pass set for an arbitrary circuit using machine learning techniques [23]. Explorations for philosophically similar problems of choosing the best candidate out of multiple choices have been performed in Ref. [5, 17, 24] using heuristics like ESP or Clifford circuits. Ref. [5] uses near-Clifford circuits for the purpose of estimating the best set of qubits to apply Dynamical Decoupling pulses to in an arbitrary circuit. Extra non-Clifford gates are needed since Dynamical Decoupling is highly qubit state-dependent.

Other than this, Clifford circuits have been extensively used as stabilizers in quantum error correction [3, 9], in quantum networks [28] and teleportation [29].

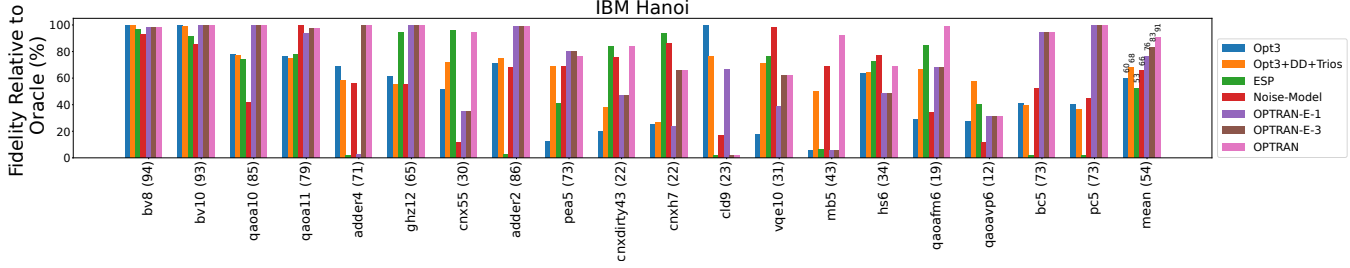


Figure 12: Fidelity relative to Oracle evaluated on IBM Hanoi.

Circuit	Qubits	Depth	Total Gates	Non Clifford Gates	Compilation [s]	Clifford Generation [s]	Simulation [s]	Device Execution Overhead
bv8	8	2-6	28-32	0	0.45	0.59	0.16	0.53x
bv10	10	2-6	28-32	0	0.55	0.83	0.15	0.53x
qaoa10	10	13-152	88-510	0	6.05	0.65	0.52	0.53x
qaoa11	11	15-69	97-395	0	4.11	0.61	0.43	0.53x
adder4	4	45-142	136-440	16-19	3.81	0.67	5.26	0.53x
ghz12	12	23-186	89-534	0	2.57	0.97	0.36	1.06x
cnx55	10	82-234	265-842	45-56	6.62	20.8	0.79	0.53x
adder2	4	32-96	10-336	14-21	2.24	0.66	0.35	0.53x
pea5	5	61-96	161-348	21-28	5.78	3.58	0.57	0.53x
cnxdirty43	8	102-329	256 - 909	52-66	7.20	11.77	0.83	0.53x
cnxh7	7	102-309	259-849	52-61	7.09	10.49	0.88	0.53x
cld9	9	83-266	283-825	45-57	7.47	26.14	0.78	0.53x
vqe10	10	28-146	161-525	26-35	3.56	0.59	0.51	0.54x
mb5	5	93-156	211-531	0-6	4.68	0.38	0.58	0.53x
hs6	6	30-73	116-318	6-8	2.21	15.2	0.40	0.73x
qaoafm6	6	61-189	199-685	27-42	5.42	21.78	0.51	20.49x
qaoavp6	6	83-157	221-536	27-33	5.08	22.14	0.75	20.81x
bc5	5	27-91	98-325	0	1.54	4.32	0.26	0.53x
pc5	5	36-104	120-366	0-6	2.67	7.57	0.33	0.53x

Table 3: Benchmark specifications and overhead for OPTRAN-E-1 on IBM Auckland. The Compilation, Clifford Generation, and Simulation Overheads are reported in seconds. The Device Execution Overhead is reported as the number of extra shots needed to run OPTRAN relative to the baseline number of shots (8192).

8. Conclusion

OPTRAN is a novel method for finding the optimal set of passes to transpile any arbitrary quantum circuit. OPTRAN first generates all possible pass combinations for a given set of input passes. The input circuit is transpiled using each of these and the post-transpilation circuits are stored. OPTRAN then generates Clifford Dummy circuits for each of these post-transpilation circuits that are executed on a simulator as well as a quantum device. Since Clifford Dummy circuits are composed entirely of Clifford gates, they are easy to simulate on classical hardware [3]. We check which pass combination did the best on the Dummy circuits by comparing the quantum device output to the ideal simulator output. Since the Dummy circuit and original circuits have an extremely similar structure and highly correlated fidelity trends for different pass combinations on a quantum device, we apply the pass combi-

nation that was optimal for the Clifford dummy circuits on the original circuit as well. Our experiments on IBM machines show that OPTRAN improves fidelity by 87.66% of the maximum possible limit over the baseline used by IBM Qiskit. We also propose low-cost variants of OPTRAN, called OPTRAN-E-3 and OPTRAN-E-1 that improve fidelity by 78.33% and 76.66% of the maximum permissible limit over the baseline at a 58.33% and 69.44% reduction in cost compared to OPTRAN, respectively.

References

- [1] Ibm quantum experience. <https://quantum-computing.ibm.com>. Accessed: 2020-11-18.
- [2] Qiskit transpiler. <https://qiskit.org/documentation/apidoc/transpiler.html>. Accessed: 2023-04-20.
- [3] Scott Aaronson and Daniel Gottesman. Improved simulation of stabilizer circuits. *Physical Review A*, 70(5):052328, 2004.
- [4] Héctor Abraham, AduOffei, Rochisha Agarwal, Ismail Yunus Akhala-waya, Gadi Aleksandrowicz, Thomas Alexander, Matthew Amy, Eli

Arbel, Arijit02, Abraham Asfaw, Artur Avkhadiev, Carlos Azaustre, AzizNgoueya, Abhik Banerjee, Aman Bansal, Panagiotis Barkoutsos, George Barron, George S. Barron, Luciano Bello, Yael Ben-Haim, Daniel Bevenius, Arjun Bhobe, Lev S. Bishop, Carsten Blank, Sorin Bolos, Samuel Bosch, Brandon, Sergey Bravyi, Bryce-Fuller, David Bucher, Artemiy Burov, Fran Cabrera, Padraig Calpin, Lauren Capel-luto, Jorge Carballo, Gines Carrascal, Adrian Chen, Chun-Fu Chen, Edward Chen, Jielun (Chris) Chen, Richard Chen, Jerry M. Chow, Spencer Churchill, Christian Claus, Christian Clauss, Romilly Cocking, Filipe Correa, Abigail J. Cross, Andrew W. Cross, Simon Cross, Juan Cruz-Benito, Chris Culver, Antonio D. Córcoles-Gonzales, Sean Dague, Tareq El Dandachi, Marcus Daniels, Matthieu Dartailh, DavideFr, Abdón Rodríguez Davila, Anton Dekusar, Delton Ding, Jun Doi, Eric Drechsler, Drew, Eugene Dumitrescu, Karel Dumon, Ivan Duran, Ka-reem EL-Safty, Eric Eastman, Grant Eberle, Pieter Eendebak, Daniel Egger, Mark Everitt, Paco Martín Fernández, Axel Hernández Ferrera, Romain Foulland, FranckChevallier, Albert Frisch, Andreas Fuhrer, Bryce Fuller, MELVIN GEORGE, Julien Gacon, Borja Godoy Gago, Claudio Gambella, Jay M. Gambetta, Adhisha Gammapila, Luis García, Tanya Garg, Shelly Garion, Austin Gilliam, Aditya Giridharan, Juan Gomez-Mosquera, Salvador de la Puente González, Jesse Gorzinski, Ian Gould, Donny Greenberg, Dmitry Grinko, Wen Guan, John A. Gunnels, Mikael Haglund, Isabel Haide, Ikko Hamamura, Omar Costa Hamido, Frank Harkins, Vojtech Havlicek, Joe Hellmers, Lukasz Herok, Stefan Hillmich, Hiroshi Horii, Connor Howington, Shaohan Hu, Wei Hu, Junye Huang, Rolf Huisman, Haruki Imai, Takashi Imamichi, Kazuaki Ishizaki, Raban Iten, Toshinari Itoko, JamesSeaward, Ali Javadi, Ali Javadi-Abhari, Jessica, Madhav Jivrajani, Kiran Johns, Scott Johnstun, Jonathan-Shoemaker, Vismai K, Tal Kachmann, Naoki Kanazawa, Kang-Bae, Anton Karazeev, Paul Kassebaum, Josh Kelso, Spencer King, Knabberjoe, Yuri Kobayashi, Arseny Kovyrshin, Rajiv Krishnakumar, Vivek Krishnan, Kevin Krsulich, Prasad Kumkar, Gawel Kus, Ryan LaRose, Enrique Lacal, Raphaël Lambert, John Lapeyre, Joe Latone, Scott Lawrence, Christina Lee, Gushu Li, Dennis Liu, Peng Liu, Yunho Maeng, Kahan Majmudar, Aleksei Malyshev, Joshua Manela, Jakub Marecek, Manoel Marques, Dmitri Maslov, Dolph Mathews, Atsushi Matsuo, Douglas T. McClure, Cameron McGarry, David McKay, Dan McPherson, Srujan Meesala, Thomas Metcalfe, Martin Mevissen, Andrew Meyer, Antonio Mezzacapo, Rohit Midha, Zlatko Minev, Abby Mitchell, Nikolaj Moll, Jhon Montanez, Michael Duane Mooring, Renier Morales, Niall Moran, Mario Motta, MrF, Prakash Murali, Jan Müggenburg, David Nadlinger, Ken Nakanishi, Giacomo Nannicini, Paul Nation, Edwin Navarro, Yehuda Naveh, Scott Wyman Neagle, Patrick Neuweiler, Johan Nicander, Pradeep Niroula, Hassi Norlen, NuoWenLei, Lee James O'Riordan, Oluwabobi Ogunbayo, Pauline Ollitrault, Raul Otaolea, Steven Oud, Dan Padilha, Hanhee Paik, Soham Pal, Yuchen Pang, Simone Perriello, Anna Phan, Francesco Piro, Marco Pistoia, Christophe Piveteau, Pierre Pocreau, Alejandro Pozas-iKerstjens, Viktor Prutyanov, Daniel Puzzuoli, Jesús Pérez, Quintii, Rafey Iqbal Rahman, Arun Raja, Nipun Ramagiri, Anirudh Rao, Rudy Raymond, Rafael Martin-Cuevas Redondo, Max Reuter, Julia Rice, Marcello La Rocca, Diego M. Rodriguez, RohithKarur, Max Rossmanek, Mingi Ryu, Tharrmarshatha SAPV, SamFerracin, Martin Sandberg, Hirmay Sandesara, Ritvik Sapra, Hayk Sargsyan, Aniruddha Sarkar, Ninad Sathaye, Bruno Schmitt, Chris Schnabel, Zachary Schoenfeld, Travis L. Scholten, Eddie Schoute, Joachim Schwarm, Ismael Faro Sertage, Kanav Seftia, Nathan Shammah, Yunong Shi, Adenilton Silva, Andrew Simonetto, Nick Singstock, Yukio Siraichi, Iskandar Situdikov, Seyon Sivarajah, Magnus Berg Sletfjerd, John A. Smolin, Matthias Soeken, Igor Olegovich Sokolov, Igor Sokolov, SooluThomas, Starfish, Dominik Steenken, Matt Stypulkoski, Shaojun Sun, Kevin J. Sung, Hitomi Takahashi, Tanvesh Takawale, Ivano Tavernelli, Charles Taylor, Pete Taylor, Soolu Thomas, Mathieu Tillet, Maddy Tod, Miroslav Tomasik, Enrique de la Torre, Kenso Trabing, Matthew Treinish, TrishaPe, Davindra Tulsi, Wes Turner, Yotam Vaknin, Carmen Recio Valcarce, Francois Varchon, Almudena Carrera Vazquez, Victor Vilal, Desirée Vogt-Lee, Christophe Vuillot, James Weaver, Johannes Weidenfeller, Rafal Wieczorek, Jonathan A. Wildstrom, Erick Winston, Jack J. Woehr, Stefan Woerner, Ryan Woo, Christopher J. Wood, Ryan Wood, Stephen Wood, Steve Wood, James Wootton, Daniyar Yeralin, David Yonge-Mallo, Richard Young, Jessie Yu, Christopher Zachow, Laura Zdanski, Helena Zhang, Christa Zoufal, Zoufalc, a kapila, a matsuo, bcamorrison, brandhsn, nick bronn, chlorophyll zz, dekel.meirom, dekelmeirom, dekool, dime10, drholmie, dtrenev, echen, elfrocampadeor, faisaldebouni, fanzzamarco, gabrieleagl, gdial, galeinston, georgios ts, gruu, hhorii, hykavitha, jagunther, jliu45, jscott2, kanejess, klinivill, krutik2966, kurarr, lerongil, ma5x, merav aharoni, michelle4654, ordmoj, sagar pahwa, rmoyard, saswati qiskit, scottkelso, sethmerkel, strickrom, sumitpuri, tigerjack, toural, tsura, crisaldo, vvilpas, welien, willhbang, yang.luh, yotamvaknibm, and Mantas Čepulkovskis. Qiskit: An open-source framework for quantum computing, 2019.

[5] Poulami Das, Swamit Tannu, Siddharth Dangwal, and Moinuddin Qureshi. Adapt: Mitigating idling errors in qubits via adaptive dynamical decoupling. In *MICRO-54: 54th Annual IEEE/ACM International Symposium on Microarchitecture*, pages 950–962, 2021.

[6] Poulami Das, Swamit Tannu, and Moinuddin Qureshi. Jigsaw: Boosting fidelity of nisq programs via measurement subsetting. In *MICRO-54: 54th Annual IEEE/ACM International Symposium on Microarchitecture*, pages 937–949, 2021.

[7] Christopher M Dawson and Michael A Nielsen. The solovay-kitaev algorithm. *arXiv preprint quant-ph/0505030*, 2005.

[8] Casey Duckering, Jonathan M Baker, Andrew Litteken, and Frederic T Chong. Orchestrated trios: compiling for efficient communication in quantum programs with 3-qubit gates. In *Proceedings of the 26th ACM International Conference on Architectural Support for Programming Languages and Operating Systems*, pages 375–385, 2021.

[9] Austin G Fowler, Matteo Mariantoni, John M Martinis, and Andrew N Cleland. Surface codes: Towards practical large-scale quantum computation. *Physical Review A*, 86(3):032324, 2012.

[10] Tudor Giurgica-Tiron, Yousef Hindy, Ryan LaRose, Andrea Mari, and William J Zeng. Digital zero noise extrapolation for quantum error mitigation. In *2020 IEEE International Conference on Quantum Computing and Engineering (QCE)*, pages 306–316. IEEE, 2020.

[11] Daniel Gottesman. The heisenberg representation of quantum computers. *arXiv preprint quant-ph/9807006*, 1998.

[12] Lov K. Grover. A fast quantum mechanical algorithm for database search. In *ANNUAL ACM SYMPOSIUM ON THEORY OF COMPUTING*, pages 212–219. ACM, 1996.

[13] Gushu Li, Yufei Ding, and Yuan Xie. Tackling the qubit mapping problem for nisq-era quantum devices. In *Proceedings of the Twenty-Fourth International Conference on Architectural Support for Programming Languages and Operating Systems*, pages 1001–1014, 2019.

[14] Guang Hao Low and Isaac L Chuang. Hamiltonian simulation by qubitization. *Quantum*, 3:163, 2019.

[15] Prakash Murali, Jonathan M Baker, Ali Javadi-Abhari, Frederic T Chong, and Margaret Martonosi. Noise-adaptive compiler mappings for noisy intermediate-scale quantum computers. In *Proceedings of the Twenty-Fourth International Conference on Architectural Support for Programming Languages and Operating Systems*, pages 1015–1029, 2019.

[16] Prakash Murali, David C McKay, Margaret Martonosi, and Ali Javadi-Abhari. Software mitigation of crosstalk on noisy intermediate-scale quantum computers. In *Proceedings of the Twenty-Fifth International Conference on Architectural Support for Programming Languages and Operating Systems*, pages 1001–1016, 2020.

[17] Paul D Nation and Matthew Treinish. Suppressing quantum circuit errors due to system variability. *arXiv preprint arXiv:2209.15512*, 2022.

[18] Joe O’Gorman and Earl T. Campbell. Quantum computation with realistic magic-state factories. *Physical Review A*, 95(3), Mar 2017.

[19] Bibek Pokharel, Namit Anand, Benjamin Fortman, and Daniel A Lidar. Demonstration of fidelity improvement using dynamical decoupling with superconducting qubits. *Physical review letters*, 121(22):220502, 2018.

[20] John Preskill. Quantum computing in the nisq era and beyond. *Quantum*, 2:79, 2018.

[21] IBM Qiskit. Pad dynamical decoupling, 2022.

[22] IBM Qiskit. Quantum device error rates, 2022.

[23] Nils Quetschlich, Lukas Burgholzer, and Robert Wille. Predicting good quantum circuit compilation options. *arXiv preprint arXiv:2210.08027*, 2022.

[24] Marie Salm, Johanna Barzen, Uwe Breitenbücher, Frank Leymann, Benjamin Weder, and Karoline Wild. The nisq analyzer: automating the selection of quantum computers for quantum algorithms. In *Symposium and Summer School on Service-Oriented Computing*, pages 66–85. Springer, 2020.

[25] Peter W. Shor. Polynomial-time algorithms for prime factorization and discrete logarithms on a quantum computer. *SIAM Journal on Computing*, 26(5):1484–1509, Oct 1997.

[26] Swamit S Tannu and Moinuddin Qureshi. Ensemble of diverse mappings. 2019.

[27] Swamit S Tannu and Moinuddin K Qureshi. Not all qubits are created equal: a case for variability-aware policies for nisq-era quantum computers. In *Proceedings of the Twenty-Fourth International Conference on Architectural Support for Programming Languages and Operating Systems*, pages 987–999, 2019.

- [28] Victor Veitch, S A Hamed Mousavian, Daniel Gottesman, and Joseph Emerson. The resource theory of stabilizer quantum computation. *New Journal of Physics*, 16(1):013009, Jan 2014.
- [29] Beni Yoshida and Norman Y Yao. Disentangling scrambling and decoherence via quantum teleportation. *Physical Review X*, 9(1):011006, 2019.